Determination of ^{111}In and ^{99m}Tc recovery in the quantification of activity with SPECT imaging*

Determinação dos fatores de recuperação do ^{111}In e do ^{99m}Tc na quantificação de atividade com imagens SPECT

Jucilene Maria Pereira[1], Joey W. Forrester[2], Maria Inês C. C. Guimarães[3], Fernando Roberto de Andrade Lima[4], Michael Gregory Stabin[5]

Abstract **OBJECTIVE: To experimentally determine the ^{99m}Tc and ^{111}In activity recovery coefficients in SPECT imaging. MATERIALS AND METHODS: Four different ^{99m}Tc and ^{111}In concentrations were utilized for quantifying activity in spheres of four different sizes. Images were obtained with a hybrid dual-head SPECT-CT imaging system. The ordered subset expectation maximization (OSEM) iterative method was utilized for images reconstruction. An attenuation map was utilized for attenuation correction, and the multiple energy window technique for scattering correction. RESULTS: Results for spheres ≤ 6 ml in volume were significantly affected by the partial volume effect. For ^{111}In quantification, results show a dependence on sphere concentrations and background levels. For ^{99m}Tc quantification, there was a tendency towards values underestimation with higher background levels. CONCLUSION: Correction factors must be utilized for compensating the partial volume effect on objects with ≤ 6 ml in volume for both radionuclides. Background subtraction to compensate spurious count present on SPECT images has a significant influence on the quantification of activity, especially for the smaller objects.**
Keywords: SPECT; ^{111}In; ^{99m}Tc; Recovery factors.

Resumo **OBJETIVO: Determinar, experimentalmente, os coeficientes de recuperação do ^{111}In e do ^{99m}Tc usando imagens SPECT. MATERIAIS E MÉTODOS: Quatro diferentes concentrações de ^{111}In e de ^{99m}Tc foram usadas para quantificar a atividade em esferas de diferentes tamanhos. As imagens foram obtidas com um equipamento híbrido SPECT/CT, com dois detectores. A reconstrução das imagens foi realizada usando o método iterativo *ordered subset expectation maximization* (OSEM). A correção de atenuação foi realizada com o uso de um mapa de atenuação e a correção de espalhamento foi realizada usando a técnica das janelas de energia. RESULTADOS: Os resultados mostraram que o efeito do volume parcial foi observado de forma mais significativa para as esferas com volume ≤ 6 ml. Para o ^{111}In, os resultados mostram uma dependência com relação às concentrações usadas nas esferas e ao nível de *background* usado. Para o ^{99m}Tc, pôde-se observar uma tendência à subestimação dos resultados quando os níveis mais altos de *background* foram utilizados. CONCLUSÃO: É necessário usar os fatores de correção para compensar o efeito do volume parcial em objetos com volume ≤ 6 ml para ambos os radionuclídeos. A subtração das contagens espúrias presentes nas imagens SPECT foi o fator que mais influenciou na quantificação da atividade nessas esferas.**
Unitermos: SPECT; ^{111}In; ^{99m}Tc; Fatores de recuperação.

Pereira JM, Forrester JW, Guimarães MICC, Lima FRA, Stabin MG. Determination of ^{111}In and ^{99m}Tc recovery in the quantification of activity with SPECT imaging. Radiol Bras. 2010;43(1):47–51.

INTRODUCTION

In nuclear medicine, the quantification of scintigraphic images[(1)] (e.g.: single photon emission computed tomography – SPECT) is used both for estimating the activity in the body of patients submitted to therapy with internal emitters, and in pharmacokinetic studies for approval of new radiopharmaceutical drugs[(2,3)].

The SPECT tomography technique allows the visualization of spatial distribution of radioactive material in the structure of interest, as it eliminates data overlap, which significantly improves the image contrast and the detection of small lesions in the patient's body.

Many authors have evaluated the accuracy in activity quantification performed with SPECT images by means of experimental studies[(4–6)], but the presented results cannot be compared, as in such studies different reconstruction methods (with different corrections), different activity values and source objects of different shapes and sizes were utilized. However, the results are in agreement with the fact that, because of the partial volume effect, the accuracy in

* Study developed at Department of Nuclear Medicine – Medical Center of Vanderbilt University, Nashville, TN, USA.

1. Master, Fellow PhD degree, Department of Nuclear Energy, Universidade Federal de Pernambuco (UFPE), Recife, PE, Brazil.

2. Bachelor, Technologist in Nuclear Medicine at Medical Center of Vanderbilt University, Nashville, TN, USA.

3. PhD, Specialist in Radiological Protection, Universidade de São Paulo (USP), São Paulo, SP, Brazil.

4. PhD, Researcher for Regional Center of Nuclear Sciences – Comissão Nacional de Energia Nuclear (CRCN-CNEN), Recife, PE, Brazil.

5. PhD, Associate Professor, Department of Radiology and Radiological Sciences – Vanderbilt University, Nashville, TN, USA.

Mailing address: Dra. Maria Inês C. C. Guimarães. Universidade de São Paulo, Faculdade de Medicina, Departamento de Radiologia. Rua Doutor Ovídio Pires de Campos, s/nº, Cerqueira César. São Paulo, SP, Brazil, 05403-010. E-mail: maria.inês@hcnet.usp.br

Received September 16, 2009. Accepted after revision December 10, 2009.

the volume and activity determination decreased when small objects (in the magnitude of 20 ml or smaller) were evaluated.

In order to characterize the error in activity quantification as a function of object size, Koral & Dewaraja[7] have systematically studied the accuracy in activity quantification (utilizing ^{131}I) as a function of the object volume, with spheres ranging from 2 to 100 cm^3. In the present study, the authors utilized the so called recovery coefficient (RC), defined by calculation of the ratio between the calculated activity and the actual activity contained in the object to evaluate the activity quantification error, and suggested the utilization of a correction factor calculated as the inverse of the recovery factor, in order to perform the activity quantification correction in small objects. The study also evidenced that the determination of such factors is influenced by the background level and by the rotation radius utilized in the image acquisition.

However, all these studies utilized ^{131}I images, as iodine is a widely utilized radionuclide, being employed both for tumors of hematologic origin, as well as for solid tumors[8].

The present study was aimed at determining the RCs in the quantification of activity for other radionuclides of interest in the clinical practice: ^{111}In and ^{99m}Tc. The first one, for being the substitute of ^{90}Y in the development of pre-therapy planning[9], and ^{99m}Tc, for being utilized in many diagnostic studies[10].

MATERIALS AND METHODS

The accuracy of activity quantification and the limits of small objects detection were evaluated not only as a function of size, but also as a function of the activity contained in the object and the presence of background activity. Initially four spheres of different external diameters – 1.5, 1.75, 2.5 and 3 cm (internal volumes of 1.4, 2.2, 6.0 and 11.5 ml, respectively) – were placed within a Jaszczak phantom (Jaszczak SPECT Phantom – Biodex Medical Systems; Shirley, NY, USA).

The experiment was carried out by first with a concentration of 74 kBq/ml in each one of the spheres, and contamination-free water in the remainder of the phantom. The activity measurement was done by using a dose calibrator model CRC-15R (Capintec Inc.; Ramsey, NJ, USA), with a resolution of 0.001 MBq, linearity of 1.1% and e accuracy of 2.8%, evaluated for the period of the development of the experiments.

In order to minimize the error associated with the measurement of low activity in the dose calibrator, the concentration was prepared by diluting 37 MBq of ^{99m}Tc in a volume of 500 ml of water. The volume necessary for each sphere was separated, obtaining the activity values of 103, 163, 444 and 850 kBq for the spheres of 1.4, 2.2, 6.0 and 11.5 ml, respectively.

The experiment was then repeated, this time adding background values corresponding to 0.5% and 1.0% of the concentration used in the spheres. For such purpose, activity values of approximately 2400 and 4800 kBq were utilized in the volume of 6393 ml of water in the Jasczak phantom. Such values are comparable to those found in a clinical situation with 0.1% and 1% of uptake for small tumors and approximately 10% uptake for other tissues distributed in an approximately uniform manner in the body. Figure 1 shows an image of the Jaszczak phantom and a side view (with the spheres positioning) obtained in the experiment carried out with ^{99m}Tc, for the condition of background equivalent to 1.0% of the concentration value utilized in the spheres.

The experiment with ^{99m}Tc was repeated for the other three values of activity concentration in the spheres: 185, 370 and 740 kBq/ml. For each concentration value, the three background conditions were repeated, corresponding to 0%, 0.5% and 1.0% of the concentrations utilized in the spheres.

The complete experiment above described was then repeated for ^{111}In, with the same activity concentrations in the spheres (74, 185, 370 and 740 kBq/ml) and for the three background conditions (0%, 0.5% and 1.0%). Thus, a total of 24 images were acquired (four different concentrations × three background levels × two radionuclides).

In each experiment the spheres were filled with a 60 ml syringe. The activity value placed in each sphere was calculated by measuring the difference of activity contained in the syringe before and after filling the sphere. Table 1 presents the reference values of activities utilized in the spheres for the acquisition of planar images and SPECT in the condition of background absence for each radionuclide.

The activity value and time of measurement were recorded and a correction for the source activity decay was made for the start time of each acquisition, with the equation 1 as follows:

$$A = A_0 \times e^{-\lambda t} \qquad (1)$$

where: A is the final activity, A_0 is the initial activity measured at the moment when the activity was placed in the sphere, λ is the radionuclide decay constant; t is the time elapsed between the moment when the activity was measured and the start of each image acquisition.

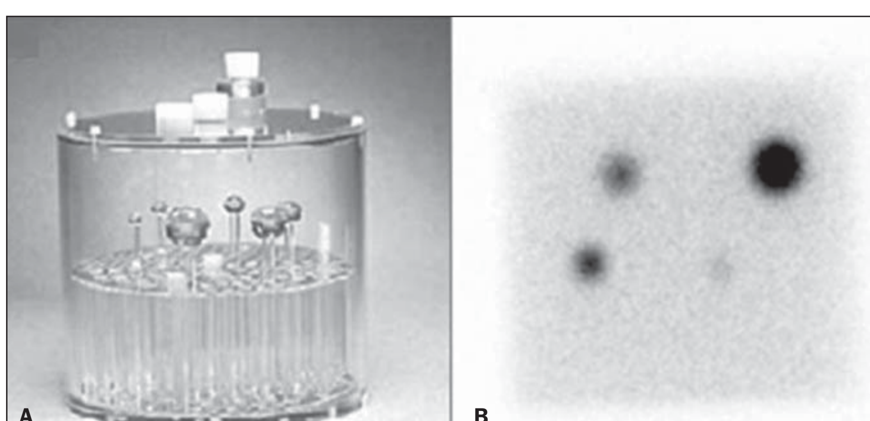

Figure 1. Image of the Jaszczak phantom utilized in the experiment (**A**) and lateral view showing the spheres positioning (**B**).

Image acquisition and reconstruction

The present study was developed at the Department of Nuclear Medicine of the Medical Center of the Vanderbilt University (MCVU), in Nashville, TN, USA. The images were acquired using a hybrid Infinia Hawkeye 4 SPECT/CT system (GE Healthcare; Milwaukee, WI, USA) with two detectors, equipped with a collimator for medium energy general purpose – MEGP for the study with ^{111}In, and for low energy general purpose – LEGP for the study with ^{99m}Tc.

The images were acquired according with the clinical protocol normally utilized at the MCVU for studies with ^{111}In and with ^{99m}Tc, with circular orbit, 360° rotation and 3° interval (step and shoot mode), matrix size of 256 × 256 pixels and a rotation radius selected to be similar to that utilized in patients' imaging. The image reconstruction was made with the iteractive method ordered subset expectation maximization (OSEM) with an iteraction and five subsets, and the image filtration was made with the Butterworth filter with a cutoff frequency of 10. An attenuation map generated before the SPECT images acquisition was utilized in the iteractive reconstruction process for the images attenuation correction. The scattering correction was made by means of the software Xeleris 2.0 (GE Healthcare; Milwaukee, WI, USA) employing energy windows defined as shown on Table 2.

The quantification of images was performed with the software ImageJ (National Institutes of Health; Bethesda, MD, USA), with regions of interest – ROIs designed on each SPECT image section utilizing the images from the attenuation map to determine the spheres size and location. The activity was determined according with equation 2.

$$A = \Sigma_{counts} \div T_{aquis} \times C_{system} \qquad (2)$$

where: Σ_{counts} corresponds to the summation of counts obtained at the ROI selected over the area of the source on each projection; T_{aquis} is the acquisition time (in seconds); C_{system} is the system calibration factor, or the count rate per activity unit ($s^{-1}.Bq^{-1}$), which was obtained from the images from a source (approximately punctual) in the air, using the same conditions (collimation, matrix size and scattering correction) employed in the images acquisition in the experiment.

Table 1 Activity reference values (kBq) utilized in the spheres, in the condition of background absence for each radionuclide.

Spheres volume	Concentrations 74 kBq/ml	185 kBq/ml	370 kBq/ml	740 kBq/ml
11.5 ml	850	2130	4255	8500
6.0 ml	444	1110	2220	4440
2.2 ml	163	410	814	1630
1.4 ml	104	260	520	1040

Table 2 Values of energy windows utilized for scattering correction.

Radionuclide	Photopeak	Scattering
^{111}In	171 keV ± 10%	125–145 keV
	245 keV ± 10%	198–208 keV
^{99m}Tc	140 keV ± 10%	122–126 keV

Definition of the ROIs and background subtraction

The size and location of the ROIs designed over the regions of the spherical sources (Figure 2) were defined from the use of images of the attenuation maps acquired for each experiment.

The background subtraction was performed as described on equation 3, with the objective of compensating the contribution of spurious counts that appear on the SPECT images after the reconstruction process. Zingerman et al.[11] have demonstrated that such contribution can be up to 12% in some images, but this depends on the size of the source and the activity in the medium where the source is immersed. It is important to highlight that such correction represents little impact on the final quantification, as it is performed only in the tomographic sections which comprise the image of the source region.

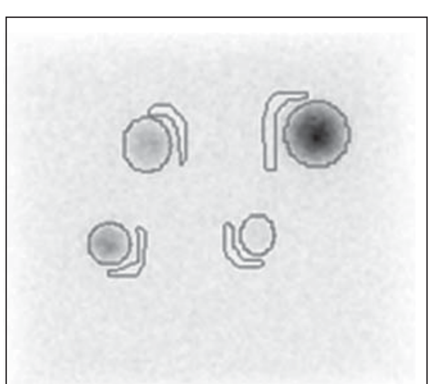

Figure 2. Examples of ROIs selected over spherical sources and selected regions for background subtraction.

$$C = C_{ROIsource} - C_{ROI.background} \times S_{source} \qquad (3)$$

where: C represents the corrected counts at the ROI over the source area; $C_{ROIsource}$ is the number of counts obtained at the ROI over the source area; $C_{ROI.background}$ is the mean value of counts by *pixel* on a selected background region near the source; S_{Source} is the area of the source in pixels.

RESULTS

The values of the calibration factors of the experimentally determined system were 80.5 $s^{-1}.MBq^{-1}$ for ^{111}In and 61.0 $s^{-1}.MBq^{-1}$ for ^{99m}Tc. In order to analyze the accuracy of the results, the calculated activity values were divided by the known activity values to determine the RCs, which are expressed as dimensionless ratios. Tables 3 and 4 present the RCs values determined for ^{111}In and ^{99m}Tc, for each sphere as a function of the used concentrations.

For ^{111}In, the results show that the RCs values were better the higher the concentration used, and were poorer the higher the used background levels were, demonstrating a dependence on these two factors.

For ^{99m}Tc, the results presented the smallest variations as compared with known activity values and did not present dependence in relation to the concentrations utilized in the spheres. However it is possible to observe a tendency to underestimate results, when the highest levels of background concentration were utilized.

As expected, the accuracy in the quantification of activity was poorer the smaller the spheres were in size, because of the partial volume effect, which was observed in a more significant manner in the spheres with a volume ≤ 6 ml. Figure 3 shows the plotted curves of the RCs reverse (1/RC), method suggested by Koral et al.[7] to correct partial volume effects as a function of the object volume. The curves were separately determined for each background level, with the RCs values presented on Tables 3 and 4.

DISCUSSION

Differently from expected, the quantification results performed with ^{111}In and ^{99m}Tc presented some discrepancies, particularly when the lower concentration (74 kBq/ml) was utilized. In this situation, the ^{111}In results were underestimated in relation to the ^{99m}Tc results. In order to analyze these results, the count densities obtained for the spheres of the same size, with the same activity concentration and inserted in the same background level for both radionuclides, were evaluated. The count densities presented similar values, however the background subtraction impact was greater for the imaging with ^{111}In. Considering that for the present experiment the background activity distribution was uniform, such difference was attributed to the contribution of scattered photons in the proximities of the source region where the $ROI_{background}$ was selected.

Only the results accuracy was evaluated, as each study was carried out only once, and it was not possible to perform the analysis of precision of such results. Thus, these images acquisition was performed in accordance with the protocol routinely employed at the MCVU, so that the conditions evaluated in the studies were close to those observed in studies with patients at such center.

Table 3 Values of recovery coefficients determined for ^{111}In as a function of concentration utilized in the spheres and of the different background levels.

Background (%)	Concentrations											
	74 kBq/ml			185 kBq/ml			370 kBq/ml			740 kBq/ml		
	0	0.5	1.0	0	0.5	1.0	0	0.5	1.0	0	0.5	1.0
11.5 ml	0.81	0.69	0.65	1.09	1.02	0.78	1.18	1.12	1.10	1.21	1.14	1.09
6.0 ml	0.64	0.44	0.45	0.85	0.84	0.57	0.93	0.91	0.78	0.92	0.92	0.77
2.2 ml	0.63	0.29	0.28	0.73	0.58	0.49	0.78	0.69	0.61	0.81	0.66	0.58
1.4 ml	0.28	0.10	0.10	0.34	0.19	0.18	0.35	0.27	0.29	0.35	0.26	0.23

Table 4 Values of recovery coefficients determined for ^{99m}Tc as a function of the concentrations utilized in the spheres and of the different background levels.

Background (%)	Concentrations											
	74 kBq/ml			185 kBq/ml			370 kBq/ml			740 kBq/ml		
	0	0.5	1.0	0	0.5	1.0	0	0.5	1.0	0	0.5	1.0
11.5 ml	0.95	0.92	0.73	1.05	1.01	0.95	1.01	0.94	0.98	1.02	1.05	1.01
6.0 ml	0.90	0.89	0.61	0.90	0.87	0.72	0.89	0.81	0.77	0.82	0.85	0.86
2.2 ml	0.67	0.51	0.54	0.69	0.74	0.62	0.65	0.69	0.49	0.70	0.69	0.60
1.4 ml	0.26	0.23	0.24	0.40	0.32	0.18	0.38	0.26	0.16	0.29	0.29	0.22

CONCLUSIONS

The present study presents the curves of the RCs reverse (1/RC) determined for ^{111}In and ^{99m}Tc as a function of the spheres volume, and for different background conditions. Previous studies presented such data only for ^{131}I. The results demonstrate the need of applying the correction to compensate for the partial volume effect on objects with a volume ≤ 6 ml for both radionuclides.

The background subtraction performed to compensate for the spurious counts effect was the factor that caused the highest uncertainty in the quantification of activ-

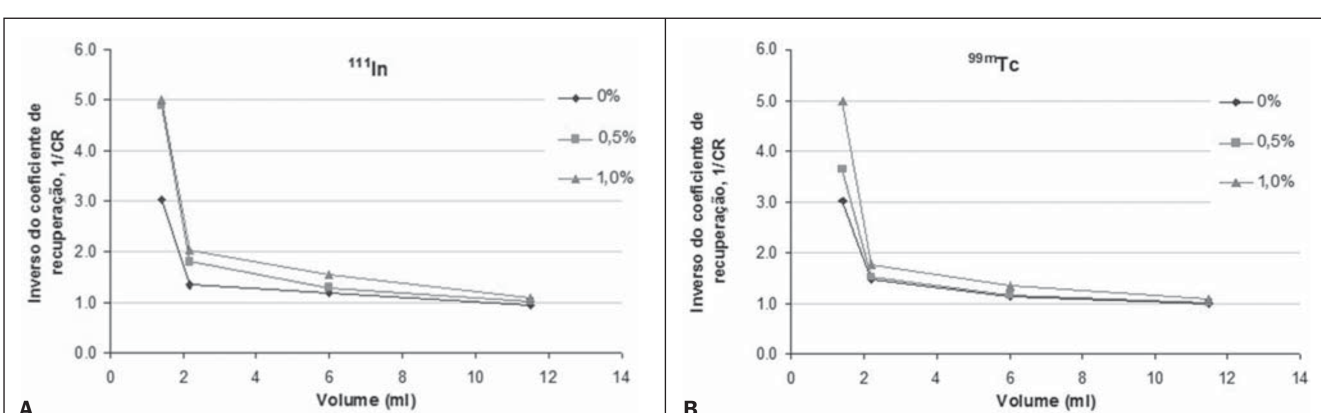

Figure 3. Curves of the recovery coefficients reverse (1/RC) determined for ^{111}In (**A**) and ^{99m}Tc (**B**) as a function of sphere volume.

ity, moreover for smaller objects. This may be corrected by carrying out a characterization of the influence of such factor on the activity quantification as a function of the object size.

REFERENCES

1. Siegel JA, Thomas SR, Stubbs JB, et al. MIRD pamphlet no. 16: Techniques for quantitative radiopharmaceutical biodistribution data acquisition and analysis for use in human radiation dose estimates. J Nucl Med. 1999;40:37S–61S.
2. Sgouros G, Squeri S, Ballangrud AM, et al. Patient-specific, 3-dimensional dosimetry in non-Hodgkin's lymphoma patients treated with ^{131}I-anti-B1 antibody: assessment of tumor dose-response. J Nucl Med. 2003;44:260–8.
3. Koral KF, Kaminski MS, Wahl RL. Correlation of tumor radiation-absorbed dose with response is easier to find in previously untreated patients. J Nucl Med. 2003;44:1541–3.
4. Jaszczak RJ, Coleman RE, Whitehead FR. Physical factors affecting quantitative measurements using camera-based single photon emission computed tomography (SPECT). IEEE Trans Nucl Sci. 1981;28:69–80.
5. Green AJ, Dewhurst SE, Begent RHJ, et al. Accurate quantification of ^{131}I distribution by gamma camera imaging. Eur J Nucl Med. 1990; 16:361–5.
6. Gilland DR, Jaszczak RJ, Turkington GT, et al. Volume and activity quantitation with iodine-123 SPECT. J Nucl Med. 1994;35:1707–13.
7. Koral KF, Dewaraja Y. I-131 SPECT activity recovery coefficients with implicit or triple-energy-window scatter correction. Nucl Instr Meth Phys Res. 1999;A422:688–92.
8. Costa LJM, Varella PCS, Del Giglio A. A utilização de anticorpos monoclonais em oncologia. [acessado em 9 de junho de 2009]. Disponível em: www.rsbcancer.com.br/rsbc/02artigo2.asp?nrev=N%BA%A02
9. Conti PS. Radioimmunotherapy with yttrium 90 ibritumomab tiuxetan (Zevalin): the role of the nuclear medicine physician. Semin Nucl Med. 2004;34:2–3.
10. Sandler MP, Coleman RE, Patton JA, et al. Diagnostic in nuclear medicine. Philadelphia: Lippincott Williams & Wilkins; 2002.
11. Zingerman Y, Golan H, Moalem A. Spatial linear recovery coefficients for quantitative evaluations in SPECT. Nucl Instr Meth Phys Res. 2009;A602: 607–13.